

Cite this: *J. Mater. Chem. C*, 2020,
8, 3795Received 19th November 2019,
Accepted 2nd February 2020

DOI: 10.1039/c9tc06334j

rsc.li/materials-c

Deviatoric stress-induced quasi-reconstructive
phase transition in ZnTe†HPSTAR
911-2020Yukai Zhuang,[‡] Lei Wu,[‡] Bo Gao,^a Zhongxun Cui,^a Huiyang Gou,^a
Dongzhou Zhang,^c Shengcai Zhu[‡] and Qingyang Hu^{‡*}

Understanding phase evolutions and the underlying mechanism under external stimuli is of fundamental importance for novel material discovery. Herein, combining angular dispersive X-ray diffraction and first-principles pathway sampling, we found that the ZnTe alloy undergoes a quasi-reconstructive transition to a metastable rocksalt phase under deviatoric stress. The rocksalt ZnTe has reconstructed chemical bonds and dendrite crystal morphology. It also suffers more severe thermodynamic hysteresis compared with the same experiments under hydrostatic pressure. However, the phase transition towards the rock-salt phase is still described by relatively small atomic displacements and is slightly first order; thus, it is neither fully displacive nor fully reconstructive. The quasi-reconstructive transition in ZnTe narrows its electronic bandgap and may provide insights into the semiconductor–metal transition in II–VI alloys in general.

Introduction

Phase transition alters the chemical, mechanical and electronic properties of materials. In chemistry and crystallography, first-order phase transitions are typically categorized into displacive transformation, which keeps the integrity of original chemical bonds, and reconstructive transformation, which is signified by the chemical bond destruction of initial structures.^{1–4} Reconstructive phase transformations constitute the most widespread type of first order phase transitions in nature, and they usually come with significant displacements of the atoms, large latent heat, sluggish transition hysteresis and evolution of crystal morphology.⁵ Despite being well-defined for most cases with proper thermodynamic controls *e.g.* external stress, two types of phase transitions can sometimes occur on the same material system.^{6,7} Intriguingly, it is possible to undergo a phase transition that owns the features of both types, thus uncovering a previously undefined “grey zone” transition between the displacive and reconstructive transition. Herein, we name this as the quasi-reconstructive transition.

In this study, we introduced zinc telluride (ZnTe) as an example of the quasi-reconstructive transition that is neither fully displacive nor reconstructive. ZnTe is a wide band gap

semiconductor which belongs to group II–VI semiconductors.⁸ It adopts the tetrahedral-coordinated (ZnTe₄) zinc blende structure (ZnTe-I, *F43m*, no. 216) at ambient conditions.⁹ Upon compression, it reconstructs into the cinnabar phase (ZnTe-II, *P3₁21*, no. 152),¹⁰ and then directly proceeds to the *Cmcm* phase (ZnTe-III, *Cmcm*, no. 63).¹¹ The structures of both ZnTe-II and ZnTe-III are regarded as distorted NaCl structures and the transformation from ZnTe-II to ZnTe-III could be classified as a first order transformation.¹² The change of bond angle and symmetry from ZnTe-II to ZnTe-III is small. Therefore, the ZnTe-II to ZnTe-III transition is regarded as a conventional displacive transformation. Under quasi-hydrostatic pressure, the five-coordinated ZnTe-III phase is stable up to 76 GPa.¹¹ The phase transition sequence of ZnTe is different from that of other zinc chalcogenides or tellurides, all of which transit *via* a six-coordinated rocksalt phase before proceeding to the *Cmcm*-type phase at high pressures.^{13–17} For ZnTe, the rocksalt-type was absent in previous high-pressure experiments.^{10,11} However, first-principles simulations predicted that rocksalt-ZnTe is metastable in the same pressure range with ZnTe-III.¹⁷ All the evidences indicate that the forbidden rocksalt-ZnTe phase may occur as a metastable phase under particular external stimuli.

In the following section, we show the results of compressed ZnTe using X-ray diffraction, Raman spectroscopy and first-principles simulations. By using non-hydrostatic pressure, we found that the alloy fell into a transition pathway towards the metastable rocksalt-phase, instead of its established transition sequence. We characterized the transition pathway on the free energy landscape and revealed the nature of its phase transitions. The non-hydrostatic environment created by deviatoric stress may enforce the transition into the quasi-reconstructive type, as we defined previously.

^a Center for High Pressure Science and Technology Research, Beijing, 100094, China. E-mail: qingyang.hu@hpstar.ac.cn

^b School of Mechatronics Engineering Guizhou Minzu University, Guiyang, 550025, China

^c Hawai'i Institute of Geophysics and Planetology, School of Ocean and Earth Science and Technology, University of Hawai'i at Manoa, Honolulu, HI, 96822, USA

^d School of Materials, Sun Yat-Sen University, Guangzhou 510275, China.
E-mail: zhushc@mail.sysu.edu.cn

† Electronic supplementary information (ESI) available. See DOI: 10.1039/c9tc06334j

‡ These authors contributed equally to this work.

Experimental

High purity ZnTe sample is commercially available through Alfa-Aesar (99.99% purity, CAS # 1315-11-3). In a symmetric diamond-anvil cell (DAC) with a pair of 300 μm anvil culets, we compressed a small piece of ZnTe up to 29 GPa to investigate its structural transition sequence. Without pressure media, non-hydrostatic conditions were used for the first set of experiments by maximizing the deviatoric stress along the compression direction. Results were compared with the same DAC setup, but a mixture of 4:1 methanol ethanol (ME) was used for pseudo-hydrostatic conditions. We collected X-ray diffraction patterns (XRD) at 13BM-C of GeoSoilEnviroCARS (GSECARS), Argonne National Laboratory (APS) to probe the structural properties.

Results and discussion

Under deviatoric stress, the phase transition from ZnTe-I to ZnTe-II occurred between the pressure range of 10.6–14.7 GPa and proceeded to the ZnTe-III phase above 14.7 GPa (Fig. 1a). The phase transition pressures were generally in the range of 2–4 GPa prior to those under quasi-hydrostatic conditions.^{18,19} The shifting of the transition pressure was previously recognized as a routine effect of deviatoric stress.²⁰ However, the volumes of ZnTe-III in our experiments under non-hydrostatic conditions were surprisingly 4.7–6.5% greater than those under quasi-hydrostatic conditions (Fig. 2a). Such great volume changes are beyond the uncertainty of pressures (Fig. S1, ESI[†]).

We extracted the lattice parameters from the two sets of experiments. Compared to the lattice parameters under hydrostatic pressure, the lattice distortion induced by deviatoric stress exhibits a significant mechanical anisotropy. As shown in Fig. 2b,

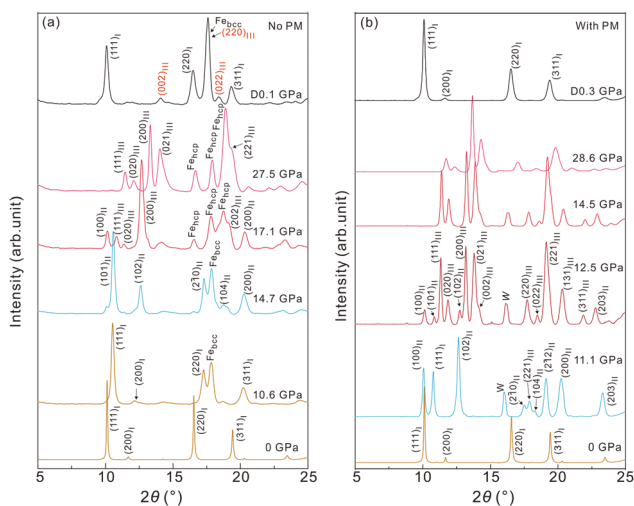


Fig. 1 Selected X-ray diffraction patterns of ZnTe under (a) non-hydrostatic ($\lambda = 0.4340 \text{ \AA}$ and extrapolated to 0.6199 \AA for clarity) and (b) quasi-hydrostatic conditions ($\lambda = 0.6199 \text{ \AA}$). Patterns of non-hydrostatic experiments include diffraction from the stainless steel gasket. The lowermost patterns in both panels were taken at ambient conditions (1 atmosphere, 293 K) outside DAC. Abbreviations: PM, pressure medium; D, decomposition.

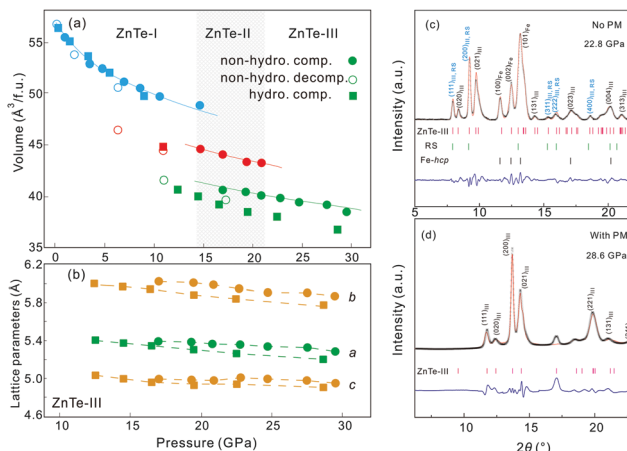


Fig. 2 (a) The volume change of ZnTe with pressure. (b) The evolution of ZnTe-III lattice parameters under non-hydrostatic (circle) and quasi-hydrostatic conditions (square), respectively. Rietveld refinement analyses of ZnTe collected at (c) 22.8 GPa under non-hydrostatic conditions ($R_1 = 0.042$ and $R_2 = 0.089$, $\lambda = 0.4340 \text{ \AA}$) and (d) 28.6 GPa under quasi-hydrostatic conditions ($R_1 = 0.055$ and $R_2 = 0.072$, $\lambda = 0.6199 \text{ \AA}$). Abbreviations: RS, rocksalt phase.

we have refined their lattice parameters and found that the volume differences were largely contributed by the stiffening of a and b axes, particularly along b . The distorted lattice may promote the displacement of atoms. The distortion may form new bonds and change atomic coordination. Due to these potential effects of lattice distortion, we were motivated to carefully track the structural changes by refining the atomic positions.

We resolved the powder diffraction patterns and extracted the atomic positions of ZnTe-III by the General Structure Analysis System (GSAS) (Fig. 2c and d).²¹ The patterns under hydrostatic conditions were readily refined as the pure ZnTe-III phase, while those under the non-hydrostatic pressure preferred the coexistence of ZnTe-III and rocksalt-ZnTe. The rocksalt phase is commonly known in II–VI semiconductors. However, in our experiments, by mixing $\sim 14.8\%$ of rocksalt-ZnTe, the refinement factor significantly improved. The refined atomic positions are summarized in Table S1 (ESI[†]), where the Zn and Te atoms apparently moved towards the b axis under non-hydrostatic conditions. As a result, the b axis is elongated by 3.7% (at 22.8 GPa). In rocksalt-ZnTe, the sets of (111), (200), (311), (222) and (400) diffractions appeared with similar d -spacings as in ZnTe-III, indicating that these specific lattice planes of both phases are highly related. Such a structural feature was absent in the hydrostatically compressed ZnTe (Fig. 2d).

The phase transition pathway, particularly the atomistic relations among ZnTe polymorphs were also characterized by first-principles simulations (details in ESI[†]). Stochastic surface walking algorithm was employed to search the nearest minima structures of ZnTe and the energetically favourable transition pathways.^{22,23} This method was successfully used to reveal the atomistic transition mechanisms of binary compounds like TiO_2 and FeO_2 .^{24,25} At 15 GPa, rocksalt-ZnTe appeared to be metastable, and it featured a six-fold Zn–Te coordination. We then calculated the energy barriers through the solid-state

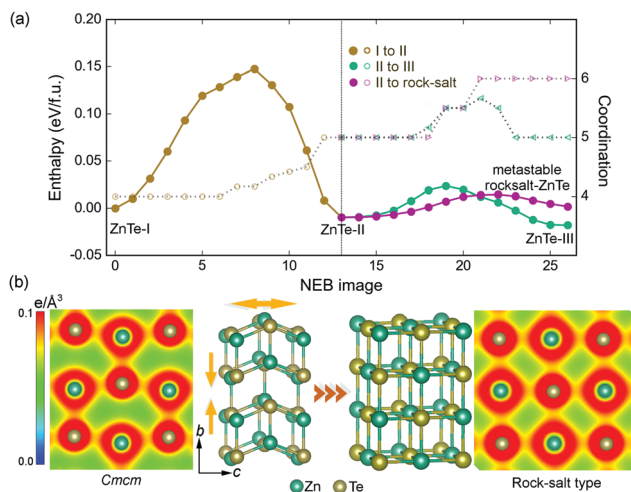


Fig. 3 Phase transition kinetics in ZnTe at 10 GPa. (a) Calculated energy barrier from ZnTe-I to II, ZnTe-II to III and ZnTe-II to rocksalt ZnTe. Hollow sphere represents the evolution of coordination numbers on the transition pathway. (b) Charge density map showing the reconstruction of atomic bonding in ZnTe-III and rocksalt ZnTe. Anisotropic compression along the *b* axis of ZnTe-III and the subsequent relaxation along *a* and *c* axes leads to the formation of 6-coordinated rocksalt ZnTe.

nudged elastic band method from 5–15 GPa (Table S2, ESI[†]).²⁶ As shown in Fig. 3, although the enthalpy of rocksalt-ZnTe at 10 GPa is 0.018 eV f.u.⁻¹ higher than that of ZnTe-III, the height of its kinetic barrier is slightly lower (24 compared to 32 meV f.u.⁻¹). This indicates that under controlled conditions, for instance, on applying deviatoric stress along the kinetically favoured direction, rocksalt-ZnTe is likely to occur as a transition intermediate.

The transition pathway from rocksalt-ZnTe to ZnTe-III is shown in Fig. S2 (ESI[†]), which is almost barrierless. Although rocksalt-ZnTe and ZnTe-III have different coordination numbers, the transition is achieved by the homogenous movements of Zn atoms along the *b* axis, thus signifying a first-order martensitic-type phase transition (Fig. 3b). Judging from the atomic displacement, the transformation to rocksalt-ZnTe is similar to the transition from ZnTe-II to ZnTe-III and therefore, is displacive-like. The applied deviatoric stress enforces the elongation of the *b* axis and steers the transition into the metastable rocksalt-ZnTe. Unlike ZnTe-III, the atomic environment in rocksalt ZnTe is well defined as six-coordinated (Fig. 3b). Based on the observation, the pressure medium might play an important role in the structural transitions. We therefore follow this track to conduct decompression and Raman spectroscopy experiments to study the bonding changes.

Upon releasing the pressure to ambient conditions, the sample in the hydrostatic environment completely reverted to ZnTe-I.²⁷ In stark contrast, the phase transitions under non-hydrostatic conditions were only partially reversible. Signature diffraction peaks of the high-pressure polymorph, including (002), (220) and (022) peaks of ZnTe-III, were still visible after the pressure was totally removed (Fig. 1, spectra at the top). Although the three diffraction peaks could not indicate the

reconstruction of the preserved ZnTe-III structure, they clearly indicated large structural hysteresis. The orthorhombic ZnTe-III lattice cell is unlikely to sustain on decreasing the pressure to the ambient pressure. However, the decompressed structure may have retained a portion of the chemical bonding of ZnTe-III.

Raman spectroscopy is more sensitive to atomic bonding and coordination.²⁸ Upon illuminating a 532 nm green laser, the Raman peaks of the ZnTe-III phase were retained when the pressure was decreased to 11.2 GPa (Fig. 4a). When the pressure was further released to 4.3 GPa, the characteristic peaks of the ZnTe-III phase (labelled as the 1, 3, 4 peaks in Fig. 4a) were still clearly visible, accompanied by a weak peak at around 225 cm⁻¹ (asterisk in Fig. 4a). At ambient pressure, Raman peaks were greatly broadened but could be generally ascribed to the coexistence of ZnTe-I and ZnTe-III. The remaining ZnTe-III peaks suggest that the sample managed to retain a portion of its bonding signatures from the high-pressure ZnTe-III under non-hydrostatic conditions. As a result, we observed that the metallic state of ZnTe-II was sustained down to 2.5 GPa (Fig. S3, ESI[†]). Such irreversibility was not observed in the hydrostatic experiments (Fig. 4b).

Raman spectroscopy measurements were repeated using silicone oil and 16:3:1 methanol-ethanol-water (MEW) as the pressure medium (Fig. S4, ESI[†]). Various pressure media were used to study the phase transition under different degrees of hydrostaticity. Depending on the solidification pressure²⁹ (Fig. S1, ESI[†]), their hydrostaticity descended from MEW to ME and then to silicone oil. By tracing the signature of Raman peaks, the shifts in the critical transition pressure were within 1 GPa and the reversibility of the phase transition was similar to that in ME. Therefore, the choice of the liquid pressure medium may impose minor effects on the phase transition pressure and irreversibility of ZnTe.

Structure reconstruction also influences the sample surface morphology,³⁰ which can be examined by a Scanning Electric

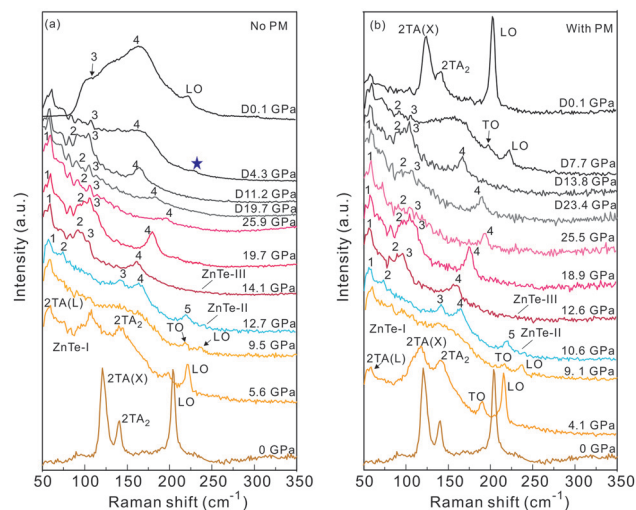


Fig. 4 Raman spectra of ZnTe under (a) non-hydrostatic and (b) quasi-hydrostatic conditions. The typical exposure time was 500 seconds for each spectrum. Intensities were properly scaled for clarity. The peak positions were read by fitting the spectra with a Lorentzian curve after removing a linear baseline. Characteristic modes of ZnTe-II and ZnTe-III are labelled in the order of increasing frequency.

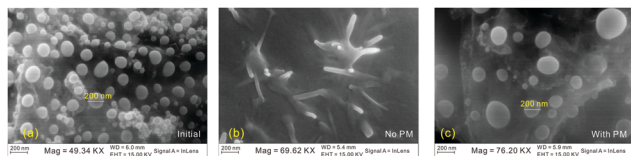


Fig. 5 (a) The SEM image of the initial sample. (b) ZnTe recovered from 25.9 GPa at non-hydrostatic conditions. (c) ZnTe recovered from 25.5 GPa at quasi-hydrostatic conditions.

Microscope (SEM). As shown in Fig. 5a, the morphology of the initial sample powder was identified as globular shaped with the average grain size of 200 nanometers (nm). Upon deviatoric stress, the decompressed sample turned into a dendritic nanostructure (Fig. 5b). The change from globular to dendritic microstructure indicates that the sample experienced a recrystallization process similar to the solidification of an eutectic alloy,³¹ which is often regarded as a temperature effect. Herein, applying an external pressure also reconstructed the crystal structure. On the other hand, under hydrostatic pressure, the sample fully recovered to the original ZnTe-I phase and retained the microscopic globular grain shape (Fig. 5c). The phase transition was fully reversible, and its morphology was also intact under hydrostatic compression.

Conclusions

In summary, we observed that ZnTe experienced anomalous compression behaviors under deviatoric stress and ZnTe evolved into a six-coordinated rocksalt structure at high pressure. Deviatoric stress pushed ZnTe to enter an alternative phase transition pathway with a lower kinetic barrier. As a result, properties belonging to the high-pressure phase became quenchable following the non-hydrostatic transition pathway. It also reconstructed the structure such that the sample was recrystallized in the compression–decompression cycle. While the small atomic displacement and the minor volume collapse are the signatures of displacive transition, the five- to six-coordination transformation, large decompression hysteresis and the recrystallized surface are ascribed to the reconstructive transition. Overall, we observed a quasi-reconstructive transformation in ZnTe under the non-hydrostatic condition. Deviatoric stress may open up opportunities to explore a modified free-energy landscape and shed new light on the transition kinetics of a wider range of materials.

Conflicts of interest

There are no conflicts to declare.

Acknowledgements

We acknowledge the use of synchrotron X-ray diffraction at the 13BM-C of GSECARS, Advanced Photon Source, Argonne National Laboratory and the BL15U1 of Shanghai Synchrotron Radiation Facility (SSRF). GeoSoilEnviroCARS is supported by the National Science Foundation – Earth Sciences (EAR – 1634415) and

Department of Energy-GeoSciences (DE-FG02-94ER14466). 13BM-C is partially supported by COMPRES under NSF Cooperative Agreement EAR-1606856. This research used resources of the Advanced Photon Source, a U.S. Department of Energy (DOE) Office of Science User Facility operated for the DOE Office of Science by Argonne National Laboratory under Contract No. DE-AC02-06CH11357. Yukai Zhuang is supported by China Postdoctoral Science Foundation with grant 18NZ021-0213-216308. Shengcai Zhu is supported by NSFC (Grant No. 21703004). Qingyang Hu is supported by NSFC (Grant No. 17N1051-0213). Operations of Center for High Pressure Science and Technology Advanced Research (HPSTAR) is partially supported by NSAF (Grant No. U1530402).

References

- 1 R. D. James, *J. Mech. Phys. Solids*, 1986, **34**, 359.
- 2 G. A. Samara, T. Sakudo and K. Yoshimitsu, *Phys. Rev. Lett.*, 1975, **35**, 1767.
- 3 K. Parlinski, Z. Q. Li and Y. Kawazoe, *Phys. Rev. Lett.*, 1997, **78**, 4063.
- 4 D. Zahn and S. Leoni, *Phys. Rev. Lett.*, 2004, **92**, 250201.
- 5 P. Tolédano and V. Dmitriev, *Reconstructive Phase Transitions: in Crystals and Quasicrystals*, World Scientific, 1996.
- 6 S. Duwal and C.-S. Yoo, *J. Phys. Chem. C*, 2016, **120**, 5101.
- 7 F. Yang, Y. Lin, J. E. Dahl, R. M. Carlson and W. L. Mao, *J. Chem. Phys.*, 2014, **141**, 154305.
- 8 S. V. Ovsyannikov and V. V. Shchennikov, *Solid State Commun.*, 2004, **132**, 333.
- 9 J.-J. Tan, G.-F. Ji, X.-R. Chen and Q.-Q. Gou, *Commun. Theor. Phys.*, 2010, **53**, 1160.
- 10 R. Franco, P. Mori-Sánchez, J. M. Recio and R. Pandey, *Phys. Rev. B: Condens. Matter Mater. Phys.*, 2003, **68**, 195208.
- 11 A. Onodera, A. Ohtani, S. Tsuduki and O. Shimomura, *Solid State Commun.*, 2008, **145**, 374.
- 12 G.-D. Lee and J. Ihm, *Phys. Rev. B: Condens. Matter Mater. Phys.*, 1996, **53**, R7622.
- 13 J. Pellicer-Porres, A. Segura, V. Muñoz, J. Zúñiga, J. P. Itié, A. Polian and P. Munsch, *Phys. Rev. B: Condens. Matter Mater. Phys.*, 2001, **65**, 012109.
- 14 J. M. Recio, M. A. Blanco, V. Luaña, R. Pandey, L. Gerward and J. Staun Olsen, *Phys. Rev. B: Condens. Matter Mater. Phys.*, 1998, **58**, 8949.
- 15 Y. Zhou, A. J. Campbell and D. L. Heinz, *J. Phys. Chem. Solids*, 1991, **52**, 821.
- 16 J. M. Recio, R. Pandey and V. V. Luana, *Phys. Rev. B: Condens. Matter Mater. Phys.*, 1993, **47**, 3401.
- 17 M. Côté, O. Zakharov, A. Rubio and M. L. Cohen, *Phys. Rev. B: Condens. Matter Mater. Phys.*, 1997, **55**, 13025.
- 18 D. Errandonea, A. Segura, D. Martínez-García and V. Muñoz-San Jose, *Phys. Rev. B: Condens. Matter Mater. Phys.*, 2009, **79**, 125203.
- 19 J. Camacho, I. Loa, A. Cantarero and K. Syassen, *High Pressure Res.*, 2002, **22**, 309.
- 20 A. E. Gleason, C. E. Quiroga, A. Suzuki, R. Pentcheva and W. L. Mao, *Earth Planet. Sci. Lett.*, 2013, **379**, 49.

- 21 A. C. Larson and R. B. V. Dreele, *Los Alamos National Laboratory Report LAUR*, 1994, pp. 86–748.
- 22 X. J. Zhang and Z. P. Liu, *J. Chem. Theory Comput.*, 2015, **11**, 4885.
- 23 C. J. Pickard and R. J. Needs, *J. Phys.: Condens. Matter*, 2011, **23**, 053201.
- 24 S.-C. Zhu, S.-H. Xie and Z.-P. Liu, *J. Am. Chem. Soc.*, 2015, **137**, 11532.
- 25 S. C. Zhu, Q. Hu, W. L. Mao, H. K. Mao and H. Sheng, *J. Am. Chem. Soc.*, 2017, **139**, 12129.
- 26 D. Sheppard, P. Xiao, W. Chemelewski, D. D. Johnson and G. Henkelman, *J. Chem. Phys.*, 2012, **136**, 074103.
- 27 A. Ohtani, M. Motobayashi and A. Onodera, *Phys. Lett. A*, 1980, **75**, 435.
- 28 C. S. Zha, H. Liu, J. S. Tse and R. J. Hemley, *Phys. Rev. Lett.*, 2017, **119**, 075302.
- 29 S. Klotz, J. C. Chervin, P. Munsch and G. L. Marchand, *J. Phys. D: Appl. Phys.*, 2009, **42**, 075413.
- 30 P. Moeck, M. Loader, M. Abdel-Hafiez and M. Hietschold, *AIP Conf. Proc.*, 2009, **1173**, 294.
- 31 M. Asle Zaeem and L. M. Hogan, *Dendritic solidification of crystals, Reference Module in Materials Science and Materials Engineering*, Elsevier, 2017.